

## Hadronic atoms in momentum space

Yong Rae Kwon and F. Tabakin

*Department of Physics and Astronomy, University of Pittsburgh, Pittsburgh, Pennsylvania 15260*

(Received 9 February 1978)

A momentum space method for hadronic atoms is developed to incorporate relativistic, nonlocal, complex hadron-nucleus interactions. The logarithmic singularity due to the Coulomb interaction has been treated by Lande's subtraction technique. Vacuum polarization, and both nuclear and pion finite-size effects have been included in this momentum space method. Precision eigenvalues and eigenfunctions for the Schrödinger, relativistic Schrödinger, Klein-Gordon (of various types), and Dirac equations have been calculated using a rapid and convenient inverse iteration method. Reliability of this novel approach is confirmed by comparing with parallel coordinate space methods. Several illustrative applications are made to simple pionic, and kaonic cases to demonstrate possible applications. For example, it is found that: (1) to extract the pion size from pionic atom data, energy shifts must be measured to an accuracy of better than 50 eV; (2) to determine the form of Klein-Gordon equations appropriate for kaonic atoms, one needs a precision of better than 20 eV; (3) the finite-range of the  $\pi$ -N interaction plays a non-negligible role and, therefore, should be carefully included in the pion-nucleus interaction. More extensive applications of these methods are suggested.

[NUCLEAR STRUCTURE Hadronic atoms, momentum space formulation, and its] applications.

### I. INTRODUCTION

A momentum space method for hadronic atom studies is presented in this paper. The goal is to develop precision methods for evaluating nonstatic, nonlocal, and relativistic effects which occur in hadronic atoms. In those atoms, the dominant effect is naturally Coulomb binding, but strong interaction information can be extracted, provided one has a flexible and precise numerical technique for including the basic hadron-nucleon interaction. This interaction is made complex to simulate the disappearance of the bound hadron into various open channels. Adopting the conventional assumption that a complex wave equation describes the dynamics, one can associate strong interaction level shifts and widths with complex energies.<sup>1,2</sup> In this way, detailed information about rather complicated nonlocal hadron-nucleus interactions at low energies can be reliably extracted.

It is clearly more convenient to treat a Coulomb interaction in coordinate, rather than in momentum space. Why then do we advocate using momentum space, which is known to be unitarily equivalent to a coordinate space description? The hope is that such a solution, although unwieldy for a Coulomb interaction, will provide a much simpler treatment of the rather complicated strong interaction dynamics. Thus, by solving a Coulomb problem in momentum space, a convenient and flexible means for studying important relativistic and nonstatic aspects of the basic hadronic probe becomes available.

Several types of dynamic hadron-nucleus effects

can be treated in momentum space, some of which are presented in this paper. For example, the finite pion-nucleon range, and associated off-shell models can be included in standard pionic atom studies. Also, the fundamental absorption mechanism, which is of paramount importance, can be examined using nonlocal operators that go beyond the over-simplified quadratic density models. For kaonic atoms, subthreshold resonances are modified by nucleon motion, by  $\Lambda$  formation<sup>3</sup> in the nuclear medium, and by nuclear binding effects, all of which require treatment of highly nonlocal operators and coupled-channel equations. Relativistic effects can also be treated conveniently in momentum space; for example, the relativistic kinetic energy operator,  $(p^2 + m^2)^{1/2} - m$ , is now quite simple. Also, the Klein-Gordon and the Dirac equations can be solved. The study of alternative relativistic equations and associated nonstatic effects is of particular interest in fundamental systems, such as charmonium,<sup>4</sup> and bound states of  $\pi^-$ -proton<sup>5</sup> and  $\pi^-$ - $\mu$ <sup>6</sup> systems. Thus many physical applications are possible using the methods presented here.

The task is therefore to cope with the Coulomb interaction in momentum space, which has a famous logarithmic singularity in each partial wave. Analytic solutions of the point-Coulomb problem are available, but do not help, since we wish to include complex, strong interaction effects. Numerous studies of the Coulomb problem in momentum space exist. One approach that appealed to us initially was to extend the Vincent-Phatak matching technique<sup>7</sup> to bound-state problems. Indeed, that idea is a practicable ap-

proach. However, a direct subtraction technique due to Alexander Lande<sup>8</sup> proved to be the simplest and clearest way to neutralize the singularity. Thus a convenient numerical solution of a long standing problem is now available, largely due to a clever subtraction step and to the availability of large computers.

In Sec. II A, we present several wave equations which can be used to specify the dynamics of hadronic atoms. These are expressed as discrete matrix problems by the introduction of a carefully designed grid of momentum points. Next (Sec. II B), the electromagnetic interaction, which means the point-Coulomb interaction modified by finite (nuclear and hadron) size and vacuum polarization effects, is shown to be readily incorporated into a momentum space numerical treatment. As a sensitive test of the procedures, various standard hadronic atom cases, which have been already treated in coordinate space, are presented. This step provides contact with past work and serves as a crucial test of the reliability of the momentum space tack. Several examples of physical applications are then offered to illustrate how one can include nonstatic effects, and as a prelude to future extensive applications, some of which are proposed in our concluding section.

## II. MOMENTUM SPACE FORMULATION

### A. Wave equations

What types of wave equations are appropriate for specifying the dynamics of hadronic atoms? For pionic and kaonic atoms, various types of Klein-Gordon equations are natural choices; whereas, for antiprotonic and sigmonic atoms, the Dirac equation is suitable. In addition, a relativistic Schrödinger equation can be defined and easily treated in momentum space and can be used for either bosons or fermions. The first wave equation to be considered is the ordinary Schrödinger equation, which serves to illustrate the approach. Once that case is understood, generalization to the relativistic Schrödinger, the Klein-Gordon, the Dirac, and coupled-channel equations follows straightforwardly. Later, we discuss how to include the electromagnetic and complex nuclear interactions.

#### Schrödinger equation

After angular momentum projection, we can write the Schrödinger equation in momentum space as a one-dimensional integral equation,

$$\frac{\hat{p}^2}{2\mu} \phi_i(\hat{p}) + \int_0^\infty v_i(\hat{p}, \hat{p}') \phi_i(\hat{p}') \hat{p}'^2 d\hat{p}' = E \phi_i(\hat{p}), \quad (1)$$

where  $\mu$  denotes the reduced mass, and  $\hat{p}$  the relative momentum. The interaction  $v_i$ , which is generally assumed to be complex, includes a Coulomb potential plus a nuclear potential. The nuclear finite size and vacuum polarization corrections are also incorporated, as discussed later.

With the properly chosen Gaussian integration points  $\hat{p}_n$ 's and weights  $w_n$ 's, Eq. (1) can be written in a discrete form

$$\frac{\hat{p}_m^2}{2\mu} \phi_i(\hat{p}_m) + \sum_{n=1}^{NP} v_{mn}^i \phi_i(\hat{p}_n) \hat{p}_n^2 w_n = E \phi_i(\hat{p}_m), \quad (2)$$

where  $v_{mn}^i \equiv v_i(\hat{p}_m, \hat{p}_n)$ , and  $NP$  denotes the number of integration points. These integration points must be carefully designed to account for the nuclear and atomic dimensions (see Appendix A). Introducing matrices,  $\hat{H}_{mn} = (\hat{p}_m^2/2\mu)\delta_{mn} + v_{mn}^i \hat{p}_n^2 w_n$  and  $\hat{\phi}_m = \phi_i(\hat{p}_m)$  for each  $l$  value, we write the Schrödinger equation in matrix form,

$$\hat{H} \hat{\phi} = E \hat{\phi}. \quad (3)$$

Note that  $\hat{H}$  can be non-Hermitian, in which case both  $\hat{\phi}$  and  $E$  are complex. The imaginary part of  $E$  is identified as one-half the level width; whereas, the real part yields the level shift.<sup>2</sup>

A method for solving the above matrix equation for bound-state problems with real, short-ranged potentials has been developed earlier.<sup>9</sup> We go beyond that work by including the long-ranged Coulomb potential and a complex nuclear potential. In addition, we employ an efficient method for finding selected complex eigenvalues and eigenfunctions (see Appendix B). The main advantage of this inverse iteration method<sup>10</sup> is that it requires only *one* inversion of a complex  $NP \times NP$  matrix, followed by simple matrix multiplications. Consequently, less computing time and core space is required compared with matrix diagonalization methods.

We now show how this inverse iteration method can be applied to other wave equations.

#### Klein-Gordon equation

Treating the hadron-nucleus plus Coulomb potential,  $V = V_N + V_C$ , as the fourth component of a four vector, we obtain one version of the Klein-Gordon equation,

$$(E - V)^2 \phi = (\hat{p}^2 c^2 + \mu^2 c^4) \phi. \quad (4)$$

This equation can be written in the form

$$[\hat{p}^2 c^2 + v(E_B)] \phi = \epsilon \phi, \quad (5)$$

where the binding energy is  $E_B = E - \mu c^2$ . The operator,  $v(E_B) = 2(E_B + \mu c^2)V - V^2$ , depends on  $E_B$ , as does the quantity  $\epsilon = E_B(E_B + 2\mu c^2)$ . The energy

dependence of the operator  $v$  prevents Eq. (5) from being a standard eigenvalue problem.

However, we can solve Eq. (5) using a simple iterative technique. A reasonable first guess  $E_1$  is used in  $v(E_1)$ , and then Eq. (5) is solved by the previously mentioned method. That process yields an eigenvalue  $\epsilon$ , from which an improved eigenvalue  $E_2$  is extracted from the relation  $\epsilon = E_2(E_2 + 2\mu c^2)$ . With the newly determined  $E_2$ ,  $v(E_2)$  is defined again and the process is repeated. For an initial guess, which is reasonably close to the actual eigenvalue, it is found that three or four iterations suffice to give an accurate eigenvalue.

The other version of the Klein-Gordon equation is obtained by treating the hadron-nucleus potential  $V_N$  as a scalar and adding it to the mass term in Eq. (4),

$$(E - V_c)^2 \phi = [p^2 c^2 + (\mu c^2 + V_N)^2] \phi, \quad (6)$$

where  $V_c$  is the electromagnetic interaction. The quadratic terms in Eqs. (4) and (6) are awkward for a nonlocal potential. Therefore, approximate forms are often used; namely,

$$(E - V_c)^2 \phi = (p^2 c^2 + \mu^2 c^4 + 2EV_N) \phi \quad (7)$$

and

$$(E - V_c)^2 \phi = (p^2 c^2 + \mu^2 c^4 + 2\mu c^2 V_N) \phi. \quad (8)$$

However, it is not necessary to make the above approximations, since the troublesome, nonlocal quadratic terms can be handled using a matrix approach. The  $V^2 \phi$  term, for a central  $V_N$ , can be written as a product of matrices

$$\begin{aligned} \langle p^2 | V^2 | \phi \rangle &= \int_0^\infty \int_0^\infty (v_i(p, p'') v_i(p'', p') p''^2 dp'') \\ &\quad \times \phi_i(p') p'^2 dp' \\ &= \sum_{n=1}^{NP} \left( \sum_{j=1}^{NP} v_{mj}^l v_{jn}^l p_j^2 w_j \right) \hat{\phi}_n p_n^2 w_n \\ &= \sum_{n=1}^{NP} \left( \sum_{j=1}^{NP} \hat{V}_{mj} \hat{V}_{jn} \right) \hat{\phi}_n = \hat{V}^2 \hat{\phi}, \end{aligned}$$

where  $\hat{V}_{mn} = v_{mn}^l p_n^2 w_n$  and  $\hat{\phi}_m = \phi_i(p_m)$ . The  $p_n$ 's and  $w_n$ 's are again the Gaussian integration points and associated weights (see Appendix A). The above procedure permits us to investigate the role of the usually neglected quadratic terms. We can also test the two forms of the Klein-Gordon equations, Eqs. (4) and (5), or their approximate forms, Eqs. (7) and (8), by applying them to kaonic atoms (see Sec. III C).

Experimental work<sup>11</sup> is underway to investigate the appropriate form for a pionic atom wave equation. Theoretically, the correct wave equation

should follow from some future basic theory, which we believe will require the methods developed here.

#### Dirac equation

In this section, we explain how the Dirac equation including a complex, nonlocal nuclear potential plus the electromagnetic interaction, can be solved numerically in momentum space. This general method can be applied to investigate various nonstatic and relativistic corrections in antiprotonic, sigmonic, and muonic atoms. The basic idea is to extend the previous discussion to a larger matrix, thereby incorporating the extra degrees of freedom. Indeed, this example demonstrates that the solution of wave equations for higher-spin particles merely requires adopting larger matrices.

The Dirac equation in momentum space involves a wave function with a large component,  $g_{i+1}(p)$ , and a small component,  $f_i(p)$ . In the  $j = l + \frac{1}{2}$  case, after angular momentum projection, the Dirac equation can be written as a coupled set

$$\begin{aligned} \int_0^\infty v_i(p, p') g_{i+1}(p') p'^2 dp' - p c f_i(p) &= E_B g_{i+1}(p), \\ \int_0^\infty v_{i+1}(p, p') f_i(p') p'^2 dp' - 2\mu c^2 f_i(p) - p c g_{i+1}(p) &= E_B f_i(p), \end{aligned} \quad (9)$$

which, in a discrete form, becomes

$$\begin{aligned} \sum_{n=1}^{NP} v_{mn}^l g_{i+1}(p_n) p_n^2 w_n - p_m c f_i(p_m) &= E_B g_{i+1}(p_m), \\ \sum_{n=1}^{NP} v_{mn}^{l+1} f_i(p_n) p_n^2 w_n - 2\mu c^2 f_i(p_m) - p_m c g_{i+1}(p_m) &= E_B f_i(p_m). \end{aligned} \quad (10)$$

For  $j = l - \frac{1}{2}$ , a similar form holds.

The coupled channel aspect of Eq. (10) can be treated readily by simply constructing complex supermatrices  $\hat{H}$  and  $\hat{\phi}$  of dimension  $2 \times NP$ :

$$\hat{H}_{mn} = \begin{cases} -v_{mn}^l p_n^2 w_n, & \text{for } m, n \leq NP \\ -p_{m-NP} c \delta_{m-NP, n}, & \text{for } m > NP, n \leq NP \\ -p_m c \delta_{m, n-NP}, & \text{for } m \leq NP, n > NP \\ -2\mu c^2 \delta_{mn} + v_{mn}^{l+1} p_{n-NP}^2 w_{n-NP}, & \text{for } m, n > NP \end{cases}$$

and

$$\hat{\phi}_n = \begin{cases} g_{i+1}(p_m), & \text{for } m \leq NP \\ f_i(p_m), & \text{for } m > NP. \end{cases}$$

The enlargement of the Hamiltonian matrix, which is introduced to include the large and small Dirac spinor components, is a simple extension of the steps used to incorporate both real and imaginary components of the wave function for the case of a complex potential. To treat particles of higher spin, a corresponding enlargement of the matrix  $H$  would be required. With the above supermatrices, a simple matrix eigenvalue problem follows, and the previously described search method is now directly applicable. Because of the coupled nature of the Dirac equation, the dimensions of the complex matrices are  $2 \times NP$ , which involves only a moderate increase in core and in computing time. It is clearly straightforward to set up the Dirac case, once one can handle the Schrödinger problem in momentum space.

#### Relativistic Schrödinger equation

One way of introducing relativistic effects from a phenomenological viewpoint is to invent a relativistic Schrödinger equation. This equation has a relativistic kinetic energy, but still involves a potential,

$$[(p^2 c^2 + \mu^2 c^4)^{1/2} - \mu c^2 + V]\phi = E\phi. \quad (11)$$

This type of equation appears in relativistic potential formulations.<sup>12</sup> In coordinate space, the operator,  $(p^2 c^2 + \mu^2 c^4)^{1/2} - \mu c^2$ , is awkward, to say the least, but it is simply a number in momentum space. Therefore, the momentum space calculation proceeds as smoothly as for the Schrödinger equation. The only change is that the  $p^2/2\mu$  term is replaced by the above kinetic energy operator. This relativistic Schrödinger equation is another viable candidate for a dynamic treatment of hadronic atoms.

#### B. Electromagnetic interaction

Having discussed several possible wave equations, let us now consider the electromagnetic interaction expressed in momentum space. Our steps are to consider first the point-Coulomb potential and then the nuclear finite size and vacuum polarization effects.

#### Point-Coulomb interaction and Lande subtraction

It is natural to use a coordinate space approach for purely local potentials. Why are we then introducing a relatively difficult method to treat the local Coulomb interaction? Interest in the momentum space formulation for the bound-state problem has been stimulated by the existence of hadronic atoms. To investigate various significant nonlocal strong interaction effects found in had-

ronic atoms, a momentum space technique is clearly desirable. To accomplish that goal, we have to sacrifice some ease in describing the point-Coulomb potential.

The hydrogenic atom problem formulated in momentum space has a long history; see, for example, early papers by Rubinstein<sup>13</sup> and Lévy.<sup>14</sup> The subsequent historical developments culminated in the Bethe-Salpeter equation for bound fermions. The search for improved formulations continues, motivated by recent developments in the positronium and charmonium systems.<sup>4</sup> In all of these developments, the main difficulty in the momentum space treatment of a bound-state problem arises from the long-ranged nature of the Coulomb potential. This long-ranged aspect causes a logarithmic singularity to appear in the Coulomb potential matrix for each orbital angular momentum  $l$ ,

$$v_l(p, p') = -\frac{Ze^2}{\pi p p'} Q_l\left(\frac{p^2 + p'^2}{2pp'}\right). \quad (12)$$

Here, the Legendre function of the second kind,  $Q_l$ , is logarithmically singular at  $p = p'$ . This singularity has recently been overcome by an ingenious subtraction technique originated by Lande. His idea is to introduce an analytically integrable quantity in the wave equation, in analogy to the principal-value subtraction done for scattering problems.<sup>9,25</sup> In particular, he introduces an integral involving the Legendre polynomial in the following steps:

$$\begin{aligned} A &\equiv \int_0^\infty v_l(p, p') \phi_l(p') p'^2 dp' \\ &= \int_0^\infty v_l(p, p') \left[ \phi_l(p') p'^2 - \frac{\phi_l(p) p^2}{P_l(z)} \right] dp' \\ &\quad + \phi_l(p) p^2 \int_0^\infty \frac{v_l(p, p')}{P_l(z)} dp', \end{aligned} \quad (13)$$

where  $z \equiv (p^2 + p'^2)/2pp'$ . Since the quantity inside the brackets in Eq. (13) vanishes linearly at the logarithmic singular point of  $v_l$ , the integrand of the first integral in Eq. (13) equals zero at  $p = p'$ . The second integral can be found analytically (see Appendix C). Thus we can write a discrete form of Eq. (13),

$$\begin{aligned} A &= \sum_{n \neq m}^{NP} v_{mn}^i \phi_l(p_n) p_n^2 w_n \\ &\quad + \phi_l(p_m) p_m^2 \left[ - \sum_{n \neq m}^{NP} \frac{v_{mn}^i w_n}{P_l[(p_m^2 + p_n^2)/2p_m p_n]} + S_l(p_m) \right], \end{aligned} \quad (14)$$

where  $S_l$  is the analytically integrable quantity,

$$S_i(p) \equiv \int_0^\infty \frac{v_i(p, p')}{P_i(z)} dp' = -\frac{Ze^2}{\pi p} \int_0^\infty \frac{Q_i(z)}{P_i(z)} \frac{dp'}{p'} \quad (15)$$

There are no diagonal matrix elements of  $v_i$  in Eq. (14). The singularity has been cured. Defining nonsingular diagonal matrix elements of  $v_i$  at our convenience,

$$v_i(p_m, p_n) \equiv \frac{1}{w_m} \left[ -\sum_{n \neq m}^{NP} \frac{v_{mn}^i w_n}{P_i[(p_m^2 + p_n^2)/2p_m p_n]} + S_i(p_m) \right], \quad (16)$$

we can simplify Eq. (14):

$$A = \sum_{n=1}^{NP} v_{mn}^i \phi_i(p_n) p_n^2 w_n,$$

which is totally free of the original singularity. The singularity has been isolated into Lande's subtraction integral,  $S_i(p)$ .

Having eliminated the singularity in the potential term, we can directly solve the eigenvalue problem, since the Hamiltonian matrix is now well behaved. The quadratic dependence of the kinetic energy term gives no numerical difficulty because of the faster fall-off of the wave function. We checked the reliability of these steps by performing calculations with various wave equations. Before presenting the results of our study, we proceed to discuss how to include nuclear finite size and vacuum polarization contributions in a momentum space treatment.

#### Nuclear finite-size effect

The extended charge distribution of the nucleus has an important effect on the energies of low-lying atomic states. This effect is quite significant for hadronic atoms, since the overlap of the hadronic wave function with the nucleus is appreciable. The Coulomb potential for an extended charge is given by

$$V_{FS}(\vec{r}) = -Ze^2 \int d\vec{r}' \frac{\rho(\vec{r}')}{|\vec{r} - \vec{r}'|}, \quad (17)$$

where the nuclear charge distribution  $\rho(\vec{r})$  is normalized according to  $\int d\vec{r} \rho(\vec{r}) = 1$ . The Fourier transform of Eq. (17) is particularly simple; namely, the Fourier transform of the point-Coulomb potential multiplied by the nuclear charge form factor  $\rho(q)$ ,

$$V_{FS}(q) = -\frac{Ze^2}{2\pi^2} \frac{\rho(q)}{q^2}. \quad (18)$$

For a given pair of momentum variables,  $p$  and  $p'$ ,

we decompose  $V_{FS}(q)$  numerically using Gaussian integration,

$$v_i^{FS}(p, p') = -\frac{Ze^2}{\pi} \int_0^\pi \frac{\rho(q)}{q^2} P_i(\cos\theta) \sin\theta d\theta. \quad (19)$$

Since the integrand in Eq. (19) is well behaved when  $p \neq p'$ , the integration can be done numerically with high precision. In the case of  $p = p'$ , careful consideration is required, because that integrand is logarithmically singular at  $\theta = 0$ . When  $\rho(q)$  is expanded near  $q = 0$ ,  $\rho(q) = \rho(0) + q^2 p(0) + \dots$ , the  $\rho(0)$  term dominates the value of the integral for  $p = p'$ . Therefore, the diagonal terms in Eq. (19) have the same logarithmic singularity as the point-Coulomb potential, which we can handle using Lande's subtraction technique. Note that any type of nuclear charge form factor may be readily employed in Eq. (19) with nominal effort. Indeed, we have used form factors for the uniform, the Fermi, and the harmonic well distributions to represent the nuclear finite size.

It is of particular importance that we can readily generalize Eq. (19) to incorporate the finite size and polarizability<sup>15</sup> of the hadrons themselves by simply multiplying Eq. (19) by the appropriate hadron form factor (see Sec. IV A, for some sample cases).

#### Vacuum polarization corrections

Vacuum polarization is well known to be significant for atomic systems. Much work<sup>16</sup> has been done to develop coordinate space potentials which incorporate the vacuum polarization irreducible diagrams. Since hadrons are located quite close to the nucleus, they are influenced by the strong electric field of the nucleus; consequently, radiative corrections for hadronic atoms are larger than for electronic atoms. Of the two radiative corrections, the self-energy and the vacuum polarization, the latter dominates in hadronic atoms, contrary to the electronic atom case. It is therefore important to include the vacuum polarization in our momentum space treatment.

For a nuclear charge distribution  $\rho(\vec{r})$ , the vacuum polarization potential to order  $\alpha Z\alpha$  is given by the Uehling potential<sup>17</sup>

$$V_2(\vec{r}) = -Ze^2 \int_1^\infty dt F_2(t) \times \left( \int d\vec{r}' \rho(\vec{r}') \frac{\exp[-(2/\lambda_e)|\vec{r} - \vec{r}'|t]}{|\vec{r} - \vec{r}'|} \right), \quad (20)$$

where

$$F_2(t) = \frac{\alpha}{\pi} \left( \frac{2}{t^2} + \frac{1}{3t^4} \right) (t^2 - 1)^{1/2}.$$

and  $\lambda_e$  denotes the reduced electron Compton wavelength. Observe that  $V_2(\vec{r})$  is a superposition of Yukawa potentials, the Fourier transform of which is trivial. Therefore we can write the momentum space expression of Eq. (20) in a simple form,

$$V_2(q) = -\frac{Ze^2}{2\pi^2} \int_1^\infty dt F_2(t) \frac{\rho(q)}{q^2 + (2t/\lambda_e)^2}. \quad (21)$$

Finite-size effects are included by keeping  $\rho(q)$  in Eq. (21). Higher-order vacuum polarization potentials, as given in the literature, are of similar structure. For example, to order  $\alpha^2 Z\alpha$ , the vacuum polarization potential in momentum space is

$$V_4(q) = -\frac{Ze^2}{2\pi^2} \int_1^\infty dt F_4(t) \frac{\rho(q)}{q^2 + (2t/\lambda_e)^2}, \quad (22)$$

where

$$F_4(t) = \left( \frac{\alpha}{\pi} \right)^2 [H(t) + G(t)],$$

$$H(t) = -(t^2 - 1)^{1/2} \left[ \frac{13}{54t^2} + \frac{7}{108t^4} + \frac{2}{9t^6} + \left( \frac{4}{3t^2} + \frac{2}{3t^4} \right) \ln[8t(t^2 - 1)] \right] + \left( \frac{44}{9t} - \frac{2}{3t^3} - \frac{5}{4t^5} - \frac{2}{9t^7} \right) \ln[t + (t^2 - 1)^{1/2}],$$

and

$$G(t) = \left( \frac{8}{3t} - \frac{2}{3t^3} \right) \int_t^\infty ds \left( \frac{3s^2 - 1}{s(s^2 - 1)} \ln[s + (s^2 - 1)^{1/2}] - (s^2 - 1)^{-1/2} \ln[8s(s^2 - 1)] \right). \quad (23)$$

This form has been extracted by Blomqvist<sup>6</sup> from the irreducible diagrams representing vacuum polarization as discussed earlier by Källen and Sabry.<sup>18</sup>

The integrands in Eqs. (21) and (22) are well behaved; therefore, both integrals can be performed numerically with high precision for a given  $q$ . The integral in Eq. (23) can be shown to be finite despite the singular integrand; here, one needs to subtract its singular aspect and treat it analytically before proceeding to numerical integration. The above vacuum polarization potentials can be projected for each  $l$  value, as done in Eq. (19).

For a point nucleus, we can replace the charge

form factor,  $\rho(q)$  in Eqs. (21) or (22) with 1. However, the effect of the nuclear finite size on the vacuum polarization can also be included easily using the steps described here. Moreover, the effect of the finite size of the hadron itself on the vacuum polarization can now be readily investigated by simply multiplying Eqs. (21) and (22) by the appropriate hadronic form factor.

### III. TEST OF THE METHOD

A momentum space method has been discussed which permits one to study various nonlocal effects that occur in hadronic atom theories. Besides the significant advantage of handling nonstatic effects, this momentum space formulation has other useful features; for example, the method includes the quadratic terms of the Klein-Gordon equation and does not resort to a perturbation method to calculate the nuclear finite size and vacuum polarization corrections. The latter point is important since such effects are not simply additive. For example, the strong interaction influences both the finite size and vacuum polarization effects via a change in the wave function. Before discussing interesting applications of this method to nonlocal and relativistic effects, we present some results that can also be calculated in coordinate space. By comparing with the corresponding coordinate space results, we can establish the accuracy and the reliability of this novel momentum space method.

#### A. Point-Coulomb interaction

To confirm the validity of Lande's subtraction method for handling the logarithmic singularity of the point-Coulomb interaction (see Appendix C), we first consider the Schrödinger, the Klein-Gordon, and the Dirac equations for a point-Coulomb interaction in momentum space using various meson masses. Numerical results obtained with a varying number of grid points are given in Table I along with exactly known energies. As the percentile errors indicate, the logarithmic singularity of the point-Coulomb interaction in momentum space can be handled accurately using Lande's subtraction method. Note that relatively few grid points are needed for very accurate and quite stable solutions. For the Klein-Gordon and Dirac equation, the accuracies obtained are comparable to those found for the Schrödinger equation. The calculated momentum space and coordinate space wave functions are found to coincide (to better than 0.1%) with the analytically known values.

TABLE I. Evaluation of the Coulomb energy in momentum space: a test of Lande's subtraction method (all energies are in keV).

Atomic state	$NP$	$E$	% error
Schrödinger equation: $E$ (exact) = -367.866			
$3d$ ( $K^-$ - $^{32}\text{S}$ )	20	-367.842	0.0065
	40	-367.866	0.0002
	60	-367.866	0.0000
Klein-Gordon equation: $E$ (exact) = -236.653			
$1S$ ( $\pi^-$ - $^{16}\text{O}$ )	20	-236.805	0.0660
	40	-236.674	0.0088
	60	-236.659	0.0027
Dirac equation: $E$ (exact) = -280.912			
$2p$ ( $\mu^-$ - $^{40}\text{Ca}$ )	20	-282.120	0.4300
	40	-280.801	0.0400
	60	-280.905	0.0029

### B. Nuclear finite size and vacuum polarization corrections

To show the versatility of the present momentum space technique, we calculated the finite-size effect for various nuclei using appropriate charge distributions. We also calculated vacuum polarization corrections to order  $\alpha^2 Z\alpha$  including the effect of nuclear finite size. Our numerical results for pionic atoms are presented in Table II, along with the charge density parameters for Gaussian and Fermi distributions, as described in Ref. 19. These momentum space results are generally quite similar to published coordinate space values. However, a precision comparison with published results is difficult since the density parameters and approximations used by various authors are not always completely specified. Nevertheless, the results in Table II, are stable, physically reasonable, and in good agreement with parallel coordinate space cases. Indeed, the stability and accuracy suggests that the momentum

space technique can be applied to a broad range of Coulomb bound-state problems.

### C. Kaon-nucleus interaction

The motivation for developing a momentum space technique is to incorporate the often complex, nonstatic hadron-nucleus interaction. For example, it is well known that for kaonic atoms the dynamics involves coupled channels and subthreshold resonances,<sup>3,20</sup> which are highly nonstatic and affected by nucleon motion. The methods presented here are ideally suited for such problems. However, to test the reliability of this method for a complex nuclear interaction, we consider first a simplified kaonic atom problem, using a local optical potential

$$V_N(q) = -\frac{1}{2\pi^2} \left( \frac{\hbar^2}{2\mu} \right) \left( 1 + \frac{m_K}{m_N} \right) \bar{a} \rho(q), \quad (24)$$

where we use  $\bar{a}$  as adjusted to fit the experiment rather than taking it to be the  $K$ - $N$  scattering length;  $\rho(q)$  is the nuclear form factor [ $\rho(0)=1$ ]. The strong interaction shifts and widths of kaonic atom levels are given in Table III, for comparison with those obtained by Koch and Sternheim.<sup>21</sup> The fitted values of the  $\bar{a}$ 's and parameters for the charge density in Ref. 21 are used for these calculations. As the results clearly show, the coordinate space results are reproduced in momentum space. Furthermore, due to the greater flexibility of the momentum space technique, we are easily able to solve the various kinds of Klein-Gordon equations using the above interaction.

The equation dependence of the strong interaction shifts and widths, for example, of the ( $3d$ - $2p$ ) transition of the  $K^-$ - $\text{S}^{32}$  atom is given in Table IV. From this table, it is clear that the inclusion of quadratic nuclear terms affects the level shifts and widths only slightly. The largest difference occurs in comparing the results using Eq. (4) to those from Eq. (6), where a level shift difference of 5 eV and a width change of 18 eV are found. These changes are negligible compared

TABLE II. Nuclear finite size and vacuum polarization corrections for pionic atoms. For  $^{12}\text{C}$ ,  $^{14}\text{N}$ , and  $^{16}\text{O}$ , we used the harmonic well density including proton size and nuclear motion as described in Ref. 19. For  $^{32}\text{S}$ ,  $^{40}\text{Ca}$ , and  $^{58}\text{Ni}$ , the standard two-parameter Fermi distribution is used. All parameters are taken from Ref. 19. Nuclear finite size is included in vacuum polarization calculations.

State	Nucleus	Density parameters (fm)	EKG (keV)	FS (keV)	VP (keV)
1s	$^{12}\text{C}$	$a = 1.64$	-132.466	-0.897	0.642
1s	$^{14}\text{N}$	$a = 1.67$	-180.773	-1.744	0.954
1s	$^{16}\text{O}$	$a = 1.76$	-236.660	-3.266	1.278
2p	$^{32}\text{S}$	$c = 3.26$ $t = 0.59$	-237.206	-0.027	0.777
2p	$^{40}\text{Ca}$	$c = 3.64$ $t = 0.57$	-371.391	-0.119	1.352
2p	$^{58}\text{Ni}$	$c = 4.28$ $t = 0.57$	-730.975	-1.151	2.409

TABLE III. Strong interaction level shifts and widths of kaonic atoms. The coordinate space results are quoted from Ref. 21. The density parameters and approximations given in Ref. 21 are also used for the momentum space calculations.

Nucleus	Level	$c$	$a$	Shift (keV)		Width (keV)	
				$r$ space	$p$ space	$r$ space	$p$ space
$^{12}\text{C}$	$2p$	2.39	0.44	0.632	0.620	1.571	1.551
$^{32}\text{S}$	$3d$	3.20	0.59	0.516	0.503	2.346	2.317

to present experimental uncertainties, but serve to illustrate the accuracy level required to ascertain which Klein-Gordon equation is appropriate.<sup>21(a)</sup> The use of a relativistic Schrödinger equation yields results very close to those found using a Klein-Gordon equation which treats the nuclear potential as the fourth component of a four vector. That Klein-Gordon equation [Eq. (4)] can be derived from the relativistic Schrödinger equation provided one neglects the commutator term  $[V, (p^2c^2 + \mu^2c^4)^{1/2}]$ . Therefore our results explicitly demonstrate that this commutator is indeed negligible for the kaonic atom case.

#### D. Complex wave functions

Wave functions for the pionic and kaonic atom cases are shown in Figs. 1 and 2. The complex wave functions are first obtained in momentum space (see Appendix B) and then subject to a Bessel transform to generate these coordinate space wave functions. The normalization was made using  $\int \psi(k)\psi(k)k^2dk = 1$ , which we believe is appropriate for the complex states we construct. That is, we interpret the states as projections of Gamow states. For a discussion of the meaning of complex eigenvalue problems and their associated normalization, we refer the reader to Ref. 2. The effect of the strong interaction is clearly seen in these wave functions; the same

TABLE IV. The wave equation dependence of the strong interaction level shift ( $\epsilon$ ) and width ( $\Gamma$ ) of the ( $4f-3d$ ) transition of  $K^-S^{32}$  atom.  $V_C$  is the Coulomb potential plus nuclear finite-size effect, and  $V_N$  is the kaon-nucleus optical potential [Eq. (24)].

Equation	$\epsilon$ (keV)	$\Gamma$ (keV)
$(\frac{p^2}{2\mu} + V_C + V_N)\phi = E_B\phi$	0.497	2.296
$(E - V_C)^2\phi = (p^2c^2 + \mu^2c^4 + 2EV_N)\phi$	0.503	2.317
$(E - V_C - V_N)^2\phi = (p^2c^2 + \mu^2c^4)\phi$	0.503	2.298
$(E - V_C)^2\phi = (p^2c^2 + \mu^2c^4 + 2\mu c^2V_N)\phi$	0.504	2.318
$(E - V_C)^2\phi = [p^2c^2 + (\mu c^2 + V_N)^2]\phi$	0.512	2.338
$[\sqrt{p^2c^2 + \mu^2c^4} + V_C + V_N]\phi = E\phi$	0.502	2.299

pattern is seen as for wave functions displayed in Refs. 1 and 20.

## IV. ILLUSTRATIVE PHYSICAL APPLICATIONS

### A. Effect of the pion finite size

It was previously asserted that the hadron finite size could be included relatively easily using momentum space. Fortunately, the form factor of the pion has recently been directly measured<sup>22</sup> yielding a rms radius of the pion  $\langle r^2 \rangle_\pi^{1/2} = (0.56 \pm 0.04)$  fm.

Is it also possible to determine the size and perhaps the polarizability of the pion indirectly from pionic atom shifts? To study this question, we take the pion form factor to be of simple Gaus-

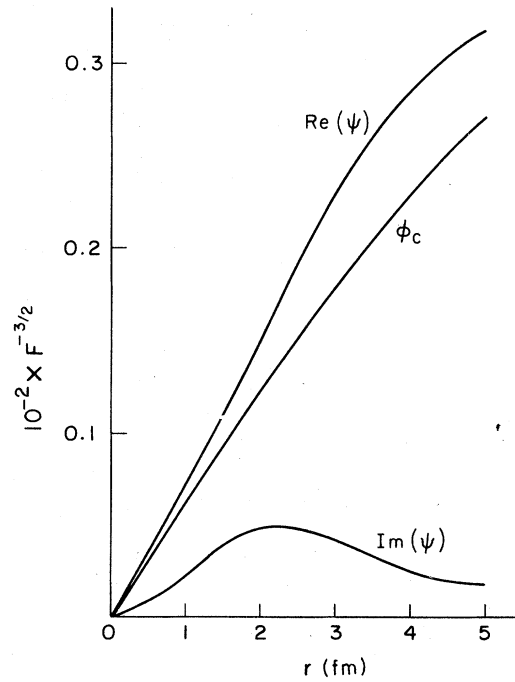


FIG. 1. The Coulomb wave function  $\phi_c(r)$  and the pion wave function  $\psi(r)$  of  $2p$  state of  $^{40}\text{Ca}$  calculated by using Eq. (26), with parameters given in Ref. 1. Wave functions are normalized with the convention  $\int \psi(k)\psi(k)k^2dk = 1$ , as discussed in Sec. III D.

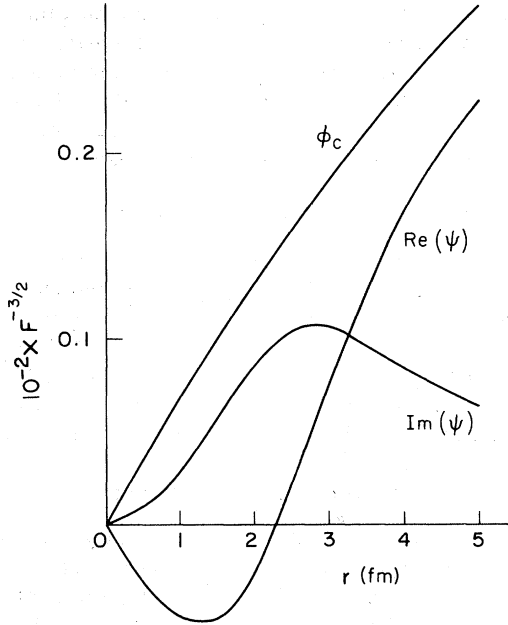


FIG. 2. The Coulomb wave function  $\phi_c(r)$  and the kaon wave function  $\psi(r)$  of  $2p$  state of  $^{12}\text{C}$  calculated by using Eq. (24) with the fitted parameter  $\bar{a} = (0.44 + 0.83i)$  fm in Ref. 21. The same normalization convention is used as in Fig. 1.

sian form

$$\rho_\pi(q) = \exp(-\langle r^2 \rangle_\pi q^2 / 6), \quad (25)$$

which gives the directly measured pion rms radius; then, we calculate the effect of the pion finite size on the Coulomb energy. The level shift due to the finite size of the pion is given in Table V, for a range of nuclei. These pion finite-size shifts vary from 4 to 5% of the shift due to the nuclear finite-size effect, with a decreasing percentage effect found for heavier nuclei. This decrease is consistent with a variation given by  $\frac{1}{2}(\langle r^2 \rangle_\pi / r_0^2) A^{-2/3}$ , as follows from a simple radius change estimate. The pion finite-size effect for  $l=0$  increases from about 6.4 to 8.7% of the vacuum polarization correction. The increase with nucleon number  $A$  follows the usual trend; that is, the finite-size change is an increasing fraction of the vacuum polarization effect for heavier nuclei.

TABLE V. Energy shifts due to pion size in pionic atoms.

State	Nucleus	Shift (eV)
1s	$^{12}\text{C}$	-41
1s	$^{14}\text{N}$	-74
1s	$^{16}\text{O}$	-120
2p	$^{32}\text{S}$	-2
2p	$^{40}\text{Ca}$	-6
2p	$^{58}\text{Ni}$	-44

TABLE VI. Effect of the finite range of the pion-nucleon interaction on shift and width of the  $(3d-2p)$  transition of  $\pi^-$ - $^{32}\text{S}$  atom.

Range (fm)	Shift (keV)	Width (keV)
0.0	0.677	0.408
0.1	0.675	0.406
0.2	0.668	0.394
0.3	0.658	0.377
0.4	0.643	0.357
0.5	0.627	0.339

The level of precision required to reliably extract information concerning hadron finite size is very high, especially when one considers other uncertainties in the hadron-nucleus interaction.<sup>15</sup>

### B. Finite range of the pion-nucleon interaction

Another application of the present method is first to treat the standard pion-nucleus optical potential of the Ericson-Ericson form<sup>23</sup> in momentum space, and then to extend it to include nonlocal effects such as arise from the short but finite range of the pion-nucleon interaction. In momentum space, the pion-nucleus optical potential can be described as

$$V_i^N(k, k') = -\frac{2\pi\hbar^2}{\mu} \left( F_i(k, k') + \frac{kk'}{2l+1} \right) \times [lH_{l-1}(k, k') + (l+1)H_{l+1}(k, k')], \quad (26)$$

where  $F_i(k, k')$  and  $H_{l\pm 1}(k, k')$  are double Bessel transforms of  $F(r)$  and  $H(r)$ , which are defined as follows:

$$F(r) \equiv b_0 A \rho(r) + b_1 [N \rho_\pi(r) - Z \rho_p(r)] + i(\text{Im} B_0) A^2 \rho^2(r),$$

$$H(r) \equiv \frac{G(r)}{1 + (4\pi/3)G(r)},$$

where

$$G(r) \equiv c_0 A \rho(r) + c_1 [N \rho_\pi(r) - Z \rho_p(r)] + i(\text{Im} C_0) A^2 \rho^2(r).$$

The conventions follow those used by Backenstoss.<sup>1</sup> It is relatively simple to extend this work to more general density dependences.<sup>24</sup> One needs only to be very careful to obtain precise double Bessel transforms, which is a manageable but nontrivial task.

To mitigate the divergence for a large  $k$  of the Kisslinger  $\vec{k} \cdot \vec{k}'$  term in the potential, we used a cutoff form  $\vec{k} \cdot \vec{k}' \exp[-\alpha^2(k^2 + k'^2)]$  with  $\alpha$  as a parameter. This parameter corresponds roughly to the finite range of the pion-nucleon interaction; equivalently, it assures a bounded or unitary pion-nucleon  $t$  matrix. As an example, the level

shift and width of the  $(3d-2p)$  transition of the  $\pi^-S^{32}$  atom is tabulated against  $\alpha$  in Table VI. A reasonable value for this range is 0.26 fm using the  $\rho$  meson mass. At this value, one finds the level shift and width change by 0.015 and 0.024 keV, respectively. The inclusion of such finite-range effects illustrates one of the major benefits of the momentum space approach as found earlier for pion scattering<sup>25</sup>; namely, to include such finite-range effects and various off-shell models. Several nonstatic, dynamic theories of the pion-nucleus interactions, such as those based on isobar doorway ideas<sup>26</sup> or  $\rho$  meson exchange,<sup>24</sup> can now be studied and tested in the pionic atom context. Such studies are planned in later work.

## V. DISCUSSION AND CONCLUSION

We have described a momentum space approach for solving complex wave equations and demonstrated its reliability and flexibility by several examples. Many interesting questions remain and we hope to stimulate interest in applying these techniques to various basic problems. Our view is to follow this work with detailed applications to pionic and kaonic atoms and to other systems.

At this stage, we already have gained some insight into the role of selected physical effects. The finite hadron size does influence the level shifts and widths in a manner consistent with elementary considerations. Also, the sensitivity to a variety of possible Klein-Gordon equations has been examined. These studies indicate that to extract hadron size, and perhaps hadron polarization information, we will need experimental precision better than 50 eV for pionic atoms. To ascertain the appropriate wave equation from an empirical viewpoint, one will need to achieve accuracies of better than 20 eV for kaonic atoms.

The finite range of the pion-nucleon interaction is seen to play a non-negligible role and should be examined further using fundamental pion-nucleus interactions. The absorption  $\rho^2(r)$  terms can be physically modified and general forms can now be examined to probe the basic absorption of pions in detail. For the charmonium problem, it is clear that momentum space offers a useful tool that might resolve some problems concerning relativistic effects and the lepton production rates.<sup>4</sup> Other interesting applications are to the basic  $\pi^-$ -proton atomic system,<sup>5</sup> to the  $\pi^-$ - $\mu$  bound state,<sup>6</sup> to new isobar models for  $\pi$  absorption, and to the  $N\bar{N}$  systems.

An overriding issue is to validate the working hypothesis that a complex wave equation stipulates the dynamics.<sup>2</sup> Clearly, one can extract widths

and shifts in other ways; indeed, basic quantum mechanical considerations suggest alternate procedures. Nevertheless, it might be possible using coupled field theory wave equations and projection operator methods to deduce that a complex wave equation problem is the appropriate description.

## ACKNOWLEDGMENTS

We wish to express our appreciation to Dr. A. Lande for providing us with detailed information about his subtraction method. We also thank Professor J. N. Bardsley, Professor C. M. Vincent, Professor R. A. Eisenstein, and Dr. G. N. Epstein for their help. This research was supported in part by the National Science Foundation.

## APPENDIX A: CHOICE OF GRID

The basic step one takes to numerically solve a wave equation in momentum space is to write it as a finite matrix equation by introducing a suitable choice of discrete integration points and weights. That choice is crucial. In coordinate-space treatments, one merely selects suitably small special increments for the well-delineated nuclear and atomic regions to achieve stable solutions of the differential equations. In the momentum space case, the choice of grid is less convenient and much care is required to assure stable solutions.

Nevertheless, to have the opportunity to examine nonlocal, relativistic, nuclear interactions, it is worthwhile to make the effort of carefully designing discrete momentum points. Therefore, despite the relative difficulty in selection of a numerical grid in momentum space, it is important to gain experience in making that selection. The guideline for selection of grid points is simply to tailor a mapping to place sufficient points where the integrand of the wave equation is significant.

To accomplish this goal, we have designed the following mapping which has the feature of giving us control over the location of points based on the nuclear and atomic dimensions. This is a sensitive matter since the atomic and nuclear regions in momentum space are not as clearly separated as they are in coordinate space. Many suitable mappings can be developed; however, we found the following form to be particularly convenient:

$$p_i = \frac{C_A \tan(\pi/4)(1+x_i)}{1 + (C_A/C_S) \tan(\pi/4)(1+x_i)}, \quad \text{for } 0 < p < C_S, \quad (\text{A1})$$

and

$$p_i = C_S + \frac{C_N \tan(\pi/4)(1+x_i)}{1 + (C_N/C_M) \tan(\pi/4)(1+x_i)}, \quad \text{for } C_S < p < C_S + C_M, \quad (\text{A2})$$

where  $x_i$ 's are standard Gaussian points defined in the interval  $(-1, 1)$ . In the above,  $C_A$  (atomic) and  $C_N$  (nuclear) control the distribution of atomic and nuclear points, respectively. Also  $C_S$  (size) is related to the "nuclear size" and  $C_M$  ( $p$  maximum) defines the largest  $p$  value associated with the smallest spacial point.  $C_M$  should be large enough not to affect the numerical results. Typical values for the pionic atom case are  $C_A = 0.02 \text{ fm}^{-1}$ ,  $C_N = 0.3 \text{ fm}^{-1}$ ,  $C_S = 0.1 \text{ fm}^{-1}$ , and  $C_M = 10^5 \text{ fm}^{-1}$ . It is often helpful to make these choices  $l$  dependent to directly include centrifugal effects.

#### APPENDIX B: INVERSE ITERATION METHOD

The momentum space approach to bound-state problems with complex nuclear interactions is made a viable numerical technique by an efficient procedure for solving for selected eigenvalues and eigenfunctions. For that purpose, an inverse iteration method, as has been suggested to us by Bardsley, is described in this appendix. Such an approach provides a key to solving bound-state problems for selected eigenvalues, since it requires low core and little computer time.

The crucial steps are to introduce a good first guess,  $\epsilon_n$ , for the desired eigenvalues, and then form a reciprocal operator,  $B_n = (H - \epsilon_n)^{-1}$ , which involves the Hamiltonian  $H$ . It is possible to construct the exact eigenvalue  $E_n$  and its eigenfunction  $|\psi_n\rangle$  by simple manipulations of the operator  $B_n$ . That procedure involves expanding an arbitrary state  $|\chi_n^0\rangle$  in the complete set  $|\psi_n\rangle$

$$|\chi_n^0\rangle = \sum_{n'} C_{n'} |\psi_{n'}\rangle,$$

and multiplying it  $N$  times by the known operator  $B_n$

$$\begin{aligned} |\chi_n^N\rangle &= B_n^N |\chi_n^0\rangle = \sum_{n'} C_{n'} (E_{n'} - \epsilon_n)^{-N} |\psi_{n'}\rangle \\ &= (E_n - \epsilon_n)^{-N} \left[ C_n |\psi_n\rangle + \sum_{n' \neq n} \left( \frac{E_n - \epsilon_n}{E_{n'} - \epsilon_n} \right)^N C_{n'} |\psi_{n'}\rangle \right]. \end{aligned} \quad (\text{B1})$$

If the energy spectrum is nondegenerate, and  $\epsilon_n$  is close to  $E_n$ , the above sum in Eq. (B1) will be dominated by one term as  $N$  increases

$$|\chi_n^N\rangle \rightarrow (E_n - \epsilon_n)^{-N} C_n |\psi_n\rangle.$$

(For a degenerate case, a linear combination of states would be extracted.) The above abstract steps can now be expressed in momentum space

$$\chi_n^N(p) \rightarrow (E_n - \epsilon_n)^{-N} C_n \psi_n(p),$$

where we can visualize the momentum  $p$  defined on a discrete grid.

In practice, we divide  $\chi_n^N(p)$  by its element with maximum modulus to avoid a possible numerical difficulty in the iteration process. Defining sequences  $\chi_n^N(p)$  and  $\tilde{\chi}_n^N(p)$  by

$$\chi_n^{N+1}(p) \equiv B_n \tilde{\chi}_n^N(p), \quad \tilde{\chi}_n^{N+1}(p) = \frac{\chi_n^{N+1}(p)}{\max[\chi_n^{N+1}(p)]}, \quad (\text{B2})$$

we have, as  $N$  increases,

$$\max[\chi_n^N(p)] = \frac{1}{E_n - \epsilon_n}, \quad \tilde{\chi}_n^N(p) = \frac{\psi_n(p)}{\max[\psi_n(p)]}.$$

Hence the desired exact eigenvalue and eigenfunction can be extracted:

$$E_n = \epsilon_n + 1/\max[\chi_n^N(p)], \quad (\text{B3})$$

and

$$\psi_n(p) = N_n \tilde{\chi}_n^N(p), \quad (\text{B4})$$

where  $N_n$  is determined by normalization. The above result is independent of the choice  $p$  and of the arbitrary starting function  $|\chi_n^0\rangle$ . Usually, a stable eigenvalue is found with  $N > 4$ . A particularly appealing feature of this approach is that the initial guess does not need to be very close to  $E_n$ .

Note that the above method is valid even when  $H$  is non-Hermitian and therefore can be used to obtain complex eigenvalues. The computer storage requirements involve mainly the complex matrix  $B_n$ , with the only algebraic steps being repeated matrix multiplications. One can also readily generalize the approach to degenerate spectra.

#### APPENDIX C: EVALUATION OF LANDE'S SUBTRACTION INTEGRAL

The logarithmic singularity due to the long-ranged Coulomb interaction has been coped with by invoking Lande's subtraction idea. Lande's observation is that a logarithmic singularity is integrable, so that one can complete the integral in Eq. (15).

Recall that the subtraction integral  $S_I$  is

$$S_I(p) = \int_0^\infty \frac{v_I(p, p')}{P_I(z)} dp' = -\frac{Ze^2}{\pi p} \int_0^\infty \frac{Q_I(z)}{P_I(z)} \frac{dp'}{p'}, \quad (\text{C1})$$

where  $Z = (p^2 + p'^2)/2pp'$ . The relation

$$Q_I(z) = \frac{1}{2} P_I(z) \ln\left(\frac{z+1}{z-1}\right) - W_{I-1}(z),$$

where

$$W_{I-1}(z) = \sum_{l'=1}^{I-1} \frac{1}{l'} P_{l'-1}(z) P_{I-l'}(z),$$

with  $W_{-1} = 0$ , permits us to isolate the logarithmic

singularity. Inserting this expression into Eq. (C1), we have

$$S_l(p) = -\frac{Ze^2}{\pi p} \left[ \frac{1}{2} \int_0^\infty \ln \left( \frac{p+p'}{p-p'} \right)^2 \frac{dp'}{p'} - \int_0^\infty \frac{W_{l-1}(z)}{P_l(z)} \frac{dp'}{p'} \right]. \quad (C2)$$

The first integral in Eq. (C2), which involves the crucial logarithmic singularity, is done analytically,

$$\int_0^\infty \ln \left( \frac{p+p'}{p-p'} \right)^2 \frac{dp'}{p'} = \pi^2. \quad (C3)$$

The second integral in Eq. (C2)

$$I_l = \frac{1}{\pi} \int_0^\infty \frac{W_{l-1}(z)}{P_l(z)} \frac{dp'}{p'} \quad (C4)$$

has a nonsingular integrand since  $z > 1$ . It can also be done analytically for each  $l$  value; for example,  $I_0 = 0$ ,  $I_1 = 1$ ,  $I_2 = (\frac{3}{2})^{1/2}$ , and  $I_3 = (8 + 5\sqrt{10})/18$ . However, for higher  $l$  values, the analytic result is

TABLE VII. Evaluation of the Lande's subtraction integral.

$$I_l = \frac{1}{\pi} \int_0^\infty \frac{W_{l-1}((p^2+p'^2)/2pp')}{P_l[(p^2+p'^2)/2pp']} \frac{dp'}{p'}$$

$l$	$I_l$	$l$	$I_l$
0	0.000 000	6	1.436 975
1	1.000 000	7	1.454 790
2	1.224 745	8	1.468 421
3	1.322 855	9	1.479 187
4	1.377 702	10	1.487 905
5	1.412 705		

rather complicated and its precise value has been determined numerically for  $l > 3$  (see Table VII).

The final result for  $S_l$  is very simple

$$S_l(p) = -\frac{Ze^2}{p} \left( \frac{\pi}{2} - I_l \right). \quad (C5)$$

This subtraction technique can be applied not only to the Schrödinger but also to the Klein-Gordon, Dirac, and various relativistic equations.

- <sup>1</sup>G. Backenstoss, *Ann. Phys. Nucl. Sci.* **20**, 467 (1970); R. Seki and C. E. Wiegand, *ibid.* **25**, 241 (1975).  
<sup>2</sup>E. C. G. Sudarshan, C. B. Chiu, and V. Gorini, *Phys. Rev. D* (to be published); G. Garcia-Calderón and R. Peierls, *Nucl. Phys.* **A265**, 443 (1976).  
<sup>3</sup>J. M. Eisenberg, *Phys. Rev. C* **14**, 2343 (1976).  
<sup>4</sup>W. Celmaster, H. Georgi, and M. Machacek: *Phys. Rev. D* **17**, 879 (1978).  
<sup>5</sup>M. Eckhause *et al.*, SREL report, 1977 (unpublished).  
<sup>6</sup>R. Coombes *et al.*, *Phys. Rev. Lett.* **37**, 249 (1976).  
<sup>7</sup>C. M. Vincent and S. C. Phatak, *Phys. Rev. C* **10**, 391 (1974).  
<sup>8</sup>A. Lande, private communication.  
<sup>9</sup>M. I. Haftel and F. Tabakin, *Phys. Rev. C* **3**, 921 (1971).  
<sup>10</sup>J. H. Wilkinson, *The Algebraic Eigenvalue Problem* (Clarendon, Oxford, 1965), p. 619.  
<sup>11</sup>P. Vogel *et al.*, LAMPF research proposal (unpublished).  
<sup>12</sup>L. L. Foldy, *Phys. Rev.* **122**, 275 (1961); L. L. Foldy and R. A. Krajcik, *Phys. Rev. Lett.* **32**, 1025 (1974); F. Coester, *Helv. Phys. Acta.* **38**, 7 (1965).  
<sup>13</sup>A. Rubinowitz, *Phys. Rev.* **73**, 1330 (1948).  
<sup>14</sup>M. Lévy, *Proc. R. Soc. (London)* **A204**, 145 (1950).  
<sup>15</sup>F. Iachello and A. Lande, *Phys. Lett.* **35B**, 205 (1971); T. E. O. Ericson and J. Hüfner, *Nucl. Phys.* **B47**, 205 (1972).  
<sup>16</sup>J. Blomqvist, *Nucl. Phys.* **B48**, 95 (1972); L. W. Ful-

- lerton and G. A. Rinker, Jr., *Phys. Rev.* **A13**, 1283 (1976); F. Roesel, D. Trautmann, and R. D. Viollier, *Nucl. Phys.* **A292**, 523 (1977).  
<sup>17</sup>E. A. Uehling, *Phys. Rev.* **48**, 55 (1935).  
<sup>18</sup>G. Källen and A. Sabry, *K. Dan. Vidensk. Selsk. Mat.-Fys. Medd.* **29**, 17 (1955).  
<sup>19</sup>L. R. B. Elton, *Nuclear Sizes* (Oxford U.P., Oxford, England, 1961).  
<sup>20</sup>M. Alberg, E. M. Henley, and L. Wilets, *Ann. Phys.* **96**, 43 (1976).  
<sup>21</sup>J. H. Koch and M. M. Sternheim, *Phys. Lett.* **28**, 1061 (1972).  
<sup>21a</sup>In the  $\pi^-$ -<sup>32</sup>S atom case, corresponding changes in level shift and width are found to be 38 and 61 eV, respectively.  
<sup>22</sup>E. B. Dally *et al.*, *Phys. Rev. Lett.* **39**, 1176 (1977).  
<sup>23</sup>M. Ericson and T. E. O. Ericson, *Ann. Phys. (N.Y.)* **36**, 323 (1966); see also G. Backenstoss in Ref. 1.  
<sup>24</sup>G. E. Brown, B. K. Jennings, and V. Rostokin, in *Proceedings of LAMPF 1977 Workshop LA-6926-C*, pl (unpublished); see also L. S. Kisslinger report, 1978 (unpublished).  
<sup>25</sup>R. Landau, S. C. Phatak, and F. Tabakin, *Ann. Phys. (N.Y.)* **78**, 299 (1973); R. A. Eisenstein and F. Tabakin, *Comp. Phys. Comm.* **12**, 237 (1976).  
<sup>26</sup>L. S. Kisslinger and W. Wang, *Ann. Phys.* **99**, 374 (1976).